

Lithium-ion Battery SOC Estimation based on GA-AUKF Algorithm

Junlin Chen*, Chun Wang

Sichuan University of Science & Engineering, School of Mechanical Engineering, Zigong, China

*Corresponding Author: Junlin Chen

ABSTRACT

Lithium-ion batteries have been widely used in the field of energy storage such as electric vehicles by virtue of their high energy density, long cycle life and environmental protection characteristics. In order to enhance the precision of battery State of Charge (SOC) estimation, this paper proposes a Thevenin model as the equivalent circuit model. Utilizing a Genetic Algorithm (GA), the model parameters are optimized to ensure the accuracy of the model. The identification results are effectively verified. On this basis, three SOC estimation algorithms, GA-EKF, GA-AEKF and GA-AUKF, were designed in this paper, and simulations and error analyses were carried out based on the UDDS operating conditions data. The results indicate that the GA-AUKF algorithm demonstrates superior accuracy and stability in terms of SOC estimation accuracy, exhibiting a significantly higher level of precision than the GA-EKF and GA-AEKF algorithms.

KEYWORDS

Lithium-ion Battery; SOC; Thevenin Model; Genetic Algorithm.

1. INTRODUCTION

In the context of the prevailing global energy crisis and mounting environmental concerns, the development of clean and efficient energy storage systems has emerged as a pivotal research area in contemporary science and technology. Lithium-ion batteries have progressively emerged as the predominant energy storage technology for electric vehicles, owing to their notable advantages, including high energy density, extended cycle life, minimal self-discharge rate, and environmental sustainability [1]. However, in practical applications, the internal parameters of Li-ion batteries fluctuate significantly with changes in external factors such as temperature, charge and discharge rates. Therefore, accurate estimation of the state of charge (SOC) of lithium-ion batteries has become one of the key issues in Battery Management System (BMS) [2].

Currently, SOC estimation methods mainly include model-based methods [3], data-driven methods [4], and hybrid methods combining the two [5]. Among them, Equivalent Circuit Model (ECM) has become the main choice in the field of SOC estimation due to its easy modelling, easy identification of parameters and its ability to better describe the dynamic characteristics of the battery [6]. For example, Gao et al. [7] highlighted a battery SOC estimation method based on an equivalent circuit model and deeply analyzed the key factors affecting the accuracy of SOC estimation. Based on the second-order equivalent circuit model and untraceable Kalman filter (UKF). In [8], An SOC estimation method based on the optimized equivalent circuit model was proposed, and the results show that the strategy can achieve high accuracy SOC estimation over a wide temperature range. Xu et al. [9] proposed a methodology that facilitates the estimation of the state of charge through the utilization of real-time capacity values derived from an equivalent circuit model. This approach

employs recursive least squares online identification of model parameters, thereby enhancing the accuracy and efficiency of the estimation process. Furthermore, scholars have innovated algorithms based on the equivalent circuit model. For instance, in [10], an enhanced SOC estimation algorithm using UKF were proposed. This algorithm overcomes the limitations of conventional SOC estimation methods, which are characterized by low accuracy, complex computation and poor robustness. The proposed algorithm demonstrates superior convergence speed and estimation accuracy in comparison to traditional methods. Guo et al. [11] proposed an enhanced SOC estimation algorithm that integrates the adaptive extended Kalman filtering (AEKF) algorithm with the PNGV equivalent circuit model to estimate the state of charge (SOC) of lithium-ion power batteries. The outcomes demonstrate the efficacy of the algorithm in accurately estimating the battery SOC in real-time. Fan et al. [12] proposed an adaptive genetic algorithm based on adaptive untraceable Kalman filtering (AUKF) to address the problem that the covariance matching window size in AUKF is susceptible to degradation of SOC estimation performance. The findings indicate that the model-based approach remains the primary focus of research at this stage, demonstrating the capability to accurately estimate the SOC of batteries.

In this paper, the GA is utilized to identify the parameters of the Thevenin model, thereby leveraging its strengths, including its robust global search capability and its good adaptability. This provides an accurate model basis for battery SOC estimation. On this basis, three SOC estimation algorithms are designed and simulation analyses and error comparisons are performed based on Urban Dynamometer Driving Schedule (UDDS) data. The findings demonstrate that the GA-AUKF algorithm demonstrates significant advantages in terms of accuracy and stability in SOC estimation, thereby effectively verifying the efficiency and reliability of the algorithm in the field of SOC estimation.

2. BATTERY MODEL PARAMETER IDENTIFICATION

2.1. Lithium-ion battery model

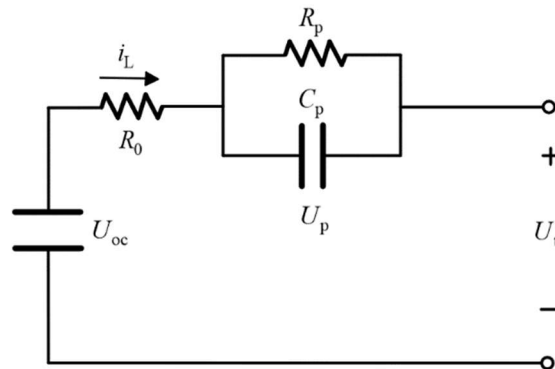


Fig. 1 Thevenin Model

Compared with electrochemical models and neural network models, equivalent circuit models are usually preferred for modelling studies of Li-ion batteries. The equivalent circuit models usually include the Rint model, the Thevenin model and the second-order RC model. In this paper, the Thevenin model is selected as the research object of lithium-ion batteries due to its advantageous characteristics, including a streamlined structure, a minimal computational effort, and a clear physical definition. Thevenin model schematic is shown in Fig. 1. The state-space equation of the Thevenin model is established as follows:

$$\begin{cases} \dot{U}_p = -\frac{1}{R_p C_p} U_p + \frac{1}{C_p} i_L \\ U_t = U_{oc} - i_L R_0 - U_p \end{cases} \quad (1)$$

Where R_0 is ohmic resistance, R_p is polarization resistance, C_p is polarization capacitance respectively, U_{oc} represents open-circuit voltage, U_t represents terminal voltage, U_p represents polarization voltage respectively. The discretization of state-space equation is obtained below:

$$\begin{cases} U_{p,k} = i_{L,k} R_p (1 - e^{-\Delta T / (R_p C_p)}) + e^{-\Delta T / (R_p C_p)} U_{p,k-1} \\ U_{t,k} = U_{oc,k} - i_{L,k} R_0 - U_{p,k} \end{cases} \quad (2)$$

Where ΔT is the sampling period, and k represent the sampling time.

2.2. Genetic Algorithm

Accurately obtaining model parameters is a key link to improve the accuracy of SOC estimation. As a stochastic search optimization method based on natural selection and genetic mechanism, Genetic Algorithm (GA) is a typical representative of evolutionary algorithms by simulating the biological evolution process and using operations such as selection, crossover and mutation to search the problem space globally. GA has significant advantages in dealing with optimization problems. In battery parameter identification, GA can be used to optimize the parameters of the battery model so that the predictions of the model are highly consistent with the actual observed data. The objective function of the GA are as follows:

$$f_{\min}(R_0, R_p, C_p) = \sum_{k=1}^n [U_{t,k} - \hat{U}_{t,k}(R_0, R_p, C_p)]^2 \quad (3)$$

Where $f_{\min}(R_0, R_p, C_p)$ is the objective function that needs to be optimized, $U_{t,k}$ is the measured terminal voltage at time k, $\hat{U}_{t,k}(R_0, R_p, C_p)$ is the estimated value of terminal voltage at time k; R_0, R_p and C_p is the parameter to be identified. In the optimization process, set the constraint range of R_0, R_p and C_p to $[10^{-6} \Omega, 10^{-2} \Omega]$, $[10^{-6} \Omega, 10^{-2} \Omega]$ and $[10F, 10^5 F]$ respectively.

First, the HPPC test data obtained in the experiment was divided into 10 data fragments to improve the accuracy of Thevenin model identification, and then genetic algorithm was used to identify the parameters of the data fragments in turn. In addition, the fitness function of GA is designed as the residual square between the predicted voltage and the measured terminal voltage. The flow of genetic algorithm based on Thevenin model is shown in Fig. 2. The specific steps of genetic algorithm are:

Step 1: Initialization

(1) Loading the experimental data of lithium-ion battery.

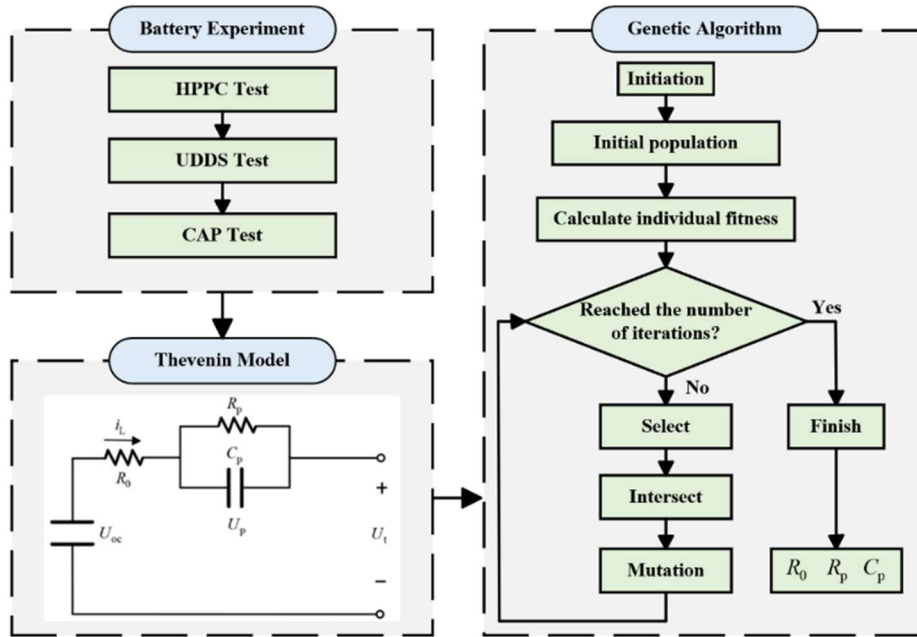


Fig. 2 Flowchart of Parameter Identification Based on Genetic Algorithms

(2) Setting key parameters of genetic algorithm.

Step 2: Complete the genetic algorithm optimization process.

(1) The initial population is randomly generated, and the model parameters are expressed as the binary code of genetic algorithm;

(2) Evaluate the fitness of the function $f(R_0) = [U_{t,k} - \hat{U}_{t,k}(R_0)]^2$ each population;

(3) Compare the size of the population generations with the set value. If the number of population generations is less than the set value, select a highly adapted population for inheritance, crossover and mutation to obtain a new population;

(4) Compare the assessment results of the new stock with those of the old stock. Return to (2);

(5) The algorithm terminates until the number of population generations is equal to the set value or the value of is greater than the constraints.

Step 3: Record the obtained optimization parameters.

2.3. The Result of Parameter Identification

Based on the HPPC experimental data and combined with the genetic algorithm steps described in the previous section, the parameter identification process of the Thevenin battery model was completed to accurately obtain the values of the model parameters ohmic resistance, polarization resistance and polarization capacitance respectively. These specific parameter values have been clearly shown in Fig. 3. Subsequently, in order to verify the accuracy and stability of the resulting model, model accuracy validation was further implemented under UDDS operating conditions. The results of the validation are shown in Fig. 4, from which it can be seen that the maximum error of the established model does not exceed 50 mV. further, by calculating that both the mean absolute error and the root mean square error of the model do not exceed 10 mV, which are 4.218 mV and 6.561 mV, respectively, it can be seen that the accuracy of the model meets the modelling requirements.

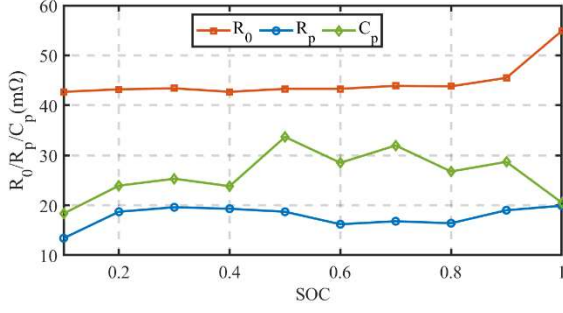


Fig. 3 Parameter Identification Results

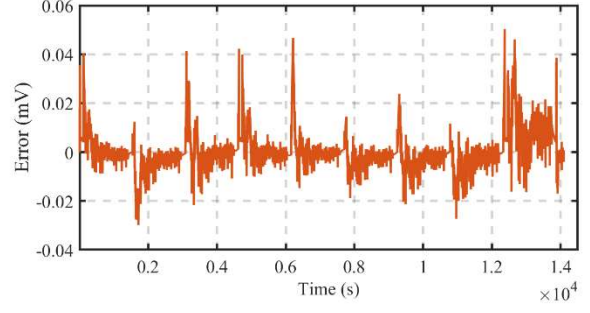


Fig. 4 Voltage Error Verification Based on UDDS Conditions

3. SOC ESTIMATION METHOD

3.1. EKF Algorithm

The extended Kalman filter (EKF) algorithm represents a state estimation technique that is widely employed for the analysis of nonlinear systems. EKF extends the traditional Kalman filter by linearizing the system dynamics and measurement model around the current estimate using a first-order Taylor series approximation. The EKF is comprised of two principal phases: prediction and update. During the prediction phase, the algorithm forecasts the state and error covariance at the subsequent time step, utilizing the nonlinear system model. In the update phase, the algorithm refines the state estimate and the error covariance. The EKF is especially efficacious in applications such as navigation, robotics, and battery SOC estimation, where system dynamics and measurements are nonlinear. The state space equation of the nonlinear discrete system for the EKF algorithm is:

$$\begin{cases} x_k = f(x_{k-1}, u_{k-1}) + \omega_{k-1} \\ y_k = h(x_k, u_k) + v_k \end{cases} \quad (4)$$

Where x_k is the state vector, u_k is the system input vector, y_k is the system input vector. ω is system noise with the covariance of Q , and v represents observation noise with the covariance of R . The state equation and observation equation are expanded by Taylor's formula to yield the following result:

$$\begin{cases} f(x_k, u_k) \approx f(\hat{x}_k, u_k) + \frac{\partial f(x_k, u_k)}{\partial \mathbf{x}_k} \Big|_{x_k = \hat{x}_k} (x_k - \hat{x}_k) \\ h(x_k, u_k) \approx h(\hat{x}_k, u_k) + \frac{\partial h(x_k, u_k)}{\partial \mathbf{x}_k} \Big|_{x_k = \hat{x}_k} (x_k - \hat{x}_k) \end{cases} \quad (5)$$

Where \hat{x}_k is the state vector estimate. The state matrix and observation matrix of the nonlinear system can be obtained through the following methodology:

$$A_k = \frac{\partial f(x_k, u_k)}{\partial \mathbf{x}_k} \Big|_{x_i = \hat{x}_i^-}, \quad C_k = \frac{\partial h(x_k, u_k)}{\partial \mathbf{x}_k} \Big|_{x_i = \hat{x}_i^-} \quad (6)$$

The linearized state and observation equations can be obtained as:

$$\begin{cases} x_k \approx A_{k-1}x_{k-1} + [f(\hat{x}_{k-1}, u_{k-1}) - A_{k-1}\hat{x}_{k-1}] + \omega_{k-1} \\ y_k \approx C_k x_k + [h(\hat{x}_k, u_k) - C_k \hat{x}_k] + v_k \end{cases} \quad (7)$$

Bringing the Thevenin model into the above equation can be expressed as:

$$\begin{cases} \begin{pmatrix} U_{p,k+1} \\ SOC_{k+1} \end{pmatrix} = \begin{pmatrix} e^{-(\Delta t/\tau)} & 0 \\ 0 & 1 \end{pmatrix} \begin{pmatrix} U_{p,k} \\ SOC_k \end{pmatrix} + \begin{pmatrix} (1 - e^{-(\Delta t/\tau)})R_p \\ \eta_i / C_{MAX} \end{pmatrix} i_{L,k} + \omega_{k-1} \\ U_{t,k} = \begin{pmatrix} -1 & \frac{\partial U_{oc}}{\partial SOC} \end{pmatrix} \begin{pmatrix} U_{p,k} \\ SOC_k \end{pmatrix} - i_{L,k} R_0 + v_k \end{cases} \quad (8)$$

3.2. AEKF Algorithm

The Adaptive Extended Kalman Filter (AEKF) algorithm is a modification of the EKF designed to improve the estimation accuracy of systems with noise characteristics or model parameters that may vary over time. The AEKF addresses the limitations of the standard EKF by dynamically adapting the process during estimation and by measuring the noise covariance matrix to reduce the effect of noise on the estimation. AEKF is widely used for battery SOC estimation. The process of adaptive noise covariance matching can be expressed in the form of an equation, designated as (9).

$$\begin{cases} F_k = \frac{1}{M} \sum_{i=k-M+1}^k e_i e_i^T \\ R_k = F_k - C_k P_k C_k^T \\ Q_k = K_k F_k K_k^T \end{cases} \quad (9)$$

Where F is the real-time estimation covariance function of the new information matrix, M is the window size. C_k is observation matrix, K_k is the Kalman gain.

3.3. AUKF algorithm

The Adaptive Unscented Kalman Filter (AUKF) is an advanced variant of the Unscented Kalman Filter (UKF) designed to enhance state estimation in nonlinear systems with varying noise characteristics or uncertain model parameters. By incorporating adaptive mechanisms, the AUKF dynamically adjusts the process and measurement noise covariance matrices, thereby enhancing its robustness to system changes and uncertainties compared to the standard UKF. The specific steps for estimating the battery SOC using the AUKF algorithm are as follows:

Step 1: Initializing the system.

$$\hat{x}_0 = E[x_0], \quad P_0 = E[(x_0 - \hat{x}_0)(x_0 - \hat{x}_0)^T] \quad (10)$$

Step 2: Completion of time and status forecast updates.

(1) Get $2n + 1$ sigma points:

$$\begin{cases} x_0 = \hat{x}, i = 0 \\ x_i = \hat{x} + (\sqrt{(n + \lambda)P})_i, i = 1, 2, 3, \dots, n \\ x_i = \hat{x} - (\sqrt{(n + \lambda)P})_{i-n}, i = n + 1, n + 2, \dots, 2n \end{cases} \quad (11)$$

(2) Updating the state variable predictions and the state variable covariance matrix:

$$\begin{cases} x_k^{i-} = f(x_{k-1}^i, u_{k-1}) \\ \hat{x}_k^- = \sum_{i=0}^{2n} \omega_i^m x_k^{i-} \\ P_k^- = \sum_{i=0}^{2n} \omega_i^c [x_k^{i-} - \hat{x}_k^-][x_k^{i-} - \hat{x}_k^-]^T + Q_{k-1} \end{cases} \quad (12)$$

(3) Calculating the sum of observations and weighted observations:

$$\begin{cases} y_k^{i-} = h(x_k^{i-}, u_k) \\ \hat{y}_k^- = \sum_{i=0}^{2n} \omega_i^m y_k^{i-} \end{cases} \quad (13)$$

(4) Calculating the variance matrix of the observation and the covariance matrix between the state quantity and the observed quantity:

$$\begin{cases} P_{yy,k} = \sum_{i=0}^{2n} \omega_i^c [y_k^{i-} - \hat{y}_k^-][y_k^{i-} - \hat{y}_k^-]^T + R_{k-1} \\ P_{xy,k} = \sum_{i=0}^{2n} \omega_i^c [x_k^{i-} - \hat{x}_k^-][y_k^{i-} - \hat{y}_k^-]^T \end{cases} \quad (14)$$

(5) Calculating the Kalman gain matrix:

$$K_k = P_{xy,k} / P_{yy,k} \quad (15)$$

(6) Updating the state vector:

$$\hat{x}_k = \hat{x}_k^- + K_k (y_k - \hat{y}_k^-) \quad (16)$$

(7) Calculating the error covariance matrix:

$$\hat{P}_{x,k}^+ = P_{x,k}^- - K_k P_{yy,k} K_k^T \quad (17)$$

(8) Complete the update of the observation noise covariance and the system noise covariance:

$$H_k = \begin{cases} \frac{k-1}{k} H_{k-1} + \frac{(y_k^- - \hat{y}_k^-)(y_k^- - \hat{y}_k^-)^T}{k} & k \leq W \\ \frac{1}{W} \sum_{i=k-W+1}^k (y_i^- - \hat{y}_i^-)(y_i^- - \hat{y}_i^-)^T & k > W \end{cases} \quad (18)$$

$$\begin{cases} R_k = H_k + K_k P_k K_k^T \\ Q_k = K_k H_k K_k^T \end{cases} \quad (19)$$

Where W is the length of the moving window, H_k is the variance.

Step 3: let $k=k+1$, $x_k = \hat{x}_k^+$, $P_k = \hat{P}_{x,k}^+$.

Step 4: Repeating step 2 to step 3 until the end of the cycle.

4. EXPERIMENTAL VERIFICATION AND ANALYSIS

4.1. Battery Experiment

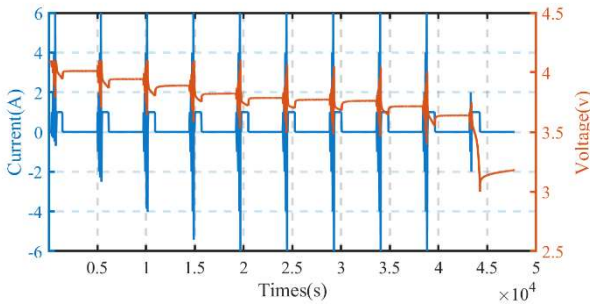


Fig. 5 Current and Voltage Data Based on HPPC Experiment

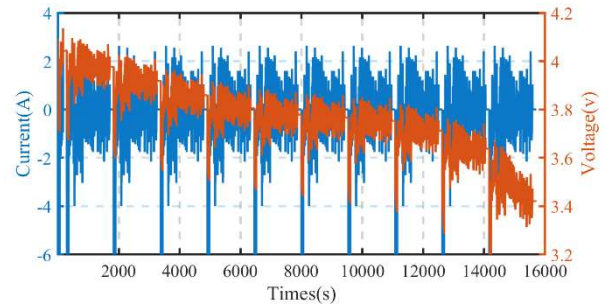


Fig. 6 Current and Voltage data Based on UDDS Experiment

In order to successfully carry out this experiment and validation work, a complete experimental platform for Battery Characterization was constructed, comprising the ARBIN BT-5HC-5V-100A test system, UUM1200 equipment and the host computer, which were integrated to perform the requisite functions. In parallel, the NMC ternary lithium-ion battery monomer was selected as the experimental research object, with the objective of exploring its dynamic characteristics. The experimental content is comprised of two principal components: the Hybrid Pulse Power Characterization test (HPPC) and the Urban Dynamometer Driving Schedule test (UDDS). During the course of the experiment, the ambient temperature was maintained at 25°C in order to ensure the stability of the test conditions. The HPPC and UDDS tests were then conducted in order to obtain the dynamic performance data of the battery. The recorded variations in current and voltage during the

experiment are illustrated in Fig. 5 and Fig. 6, which provides a clear demonstration of the battery's response behaviour under the HPPC and UDDS test conditions.

4.2. Experimental Results and Analysis

In this paper, the ampere-time integration method is chosen to define the SOC of lithium-ion batteries, and it is used as the reference SOC value. The formula for this method is shown in equation (20).

$$SOC_t = SOC_0 - \frac{1}{C_M} \int_0^t \eta I dt \quad (20)$$

where C_M is the maximum capacity of the Li-ion battery; η is the charge-discharge efficiency; I is the charge-discharge current.

In the stage of experimental analysis, the UDDS working condition data is selected at 25°C to simulate and verify the proposed method. The SOC estimation results and estimation errors based on the GA-EKF, GA-AEKF and GA-AUKF algorithms are shown in Fig. 7. From the figure, it can be observed that the estimation results are stable and the error fluctuation range is small, indicating that all three filtering algorithms have good adaptability to the characteristics of lithium-ion batteries.

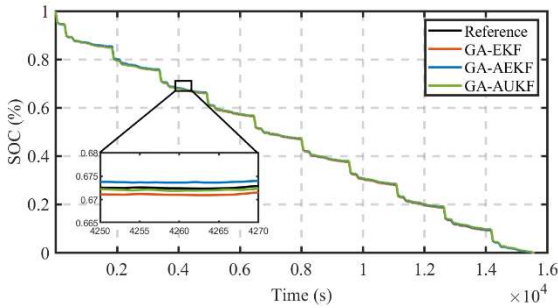


Fig. 7 SOC Estimation Results

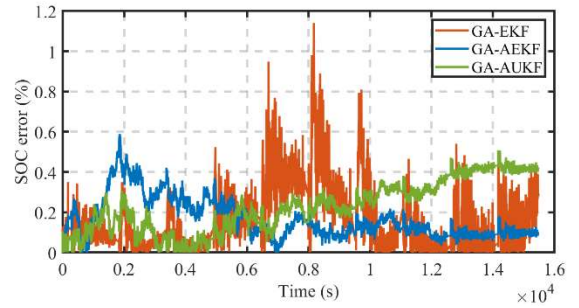


Fig. 8 SOC Estimation Error Results

In this section, the SOC estimation error is taken as an absolute value and the results are plotted as shown in Fig. 8. It is clear from the figure that the maximum error of all three algorithms is less than 1.2%, indicating their good adaptability and robustness in SOC estimation for Li-Ion batteries. Regarding the performance of the individual algorithms, the GA-EKF algorithm has a large error fluctuation, while the GA-AEKF and GA-AUKF algorithms have a relatively stable performance with maximum errors controlled below 0.6%. To analyze the reason, the GA-AEKF and GA-AUKF algorithms adaptively adjust the noise in the structure, which reduces the influence of the noise on the SOC estimation more effectively and improves the estimation accuracy compared to the GA-EKF algorithm. In addition, the SOC estimation error based on the GA-AEKF algorithm gradually decreases with the increase of SOC, showing good dynamic response characteristics, while the SOC estimation error based on the GA-AUKF algorithm shows a trend of gradual increase, reflecting the applicability characteristics of different algorithms in different SOC ranges. Taken together, the GA-AEKF and GA-AUKF algorithms have significant advantages in terms of SOC estimation accuracy and stability.

$$MAX = \max(\hat{SOC}_i - SOC_{real,i}) \quad (21)$$

$$\text{MAE} = \frac{1}{N} \sum_{i=1}^N (\hat{\text{SOC}}_i - \text{SOC}_{\text{real},i}) \quad (22)$$

$$\text{RMSE} = \sqrt{\frac{1}{N} \sum_{i=1}^N (\hat{\text{SOC}}_i - \text{SOC}_{\text{real},i})^2} \quad (23)$$

Furthermore, in order to quantitatively assess the accuracy of the three filtering algorithms, EKF, AEKF and AUKF, the Maximum Absolute Error (MAX), the Mean Absolute Error (MAE) and the Root Mean Squared Error (RMSE) are selected as the evaluation indexes, the specific formulae are shown in equations (21)-(22). The accuracy of the SOC estimation provided by the three algorithms is evaluated using the aforementioned error indicators, with the results presented in Fig. 9. As demonstrated in Figure, a comparison of MAX metrics reveals that the maximum error based on the GA-EKF algorithm reaches 1.14%, while the maximum error of both GA-AEKF and GA-AUKF algorithms does not exceed 0.6%. This observation signifies a substantial reduction in the magnitude of the error. Furthermore, under the MAE evaluation framework, the estimation errors of GA-AEKF and GA-AUKF algorithms were reduced by 6.2% and 7.0%, respectively, in comparison to the GA-EKF algorithm, which demonstrated superior estimation accuracy. A similar outcome was observed when the RMSE index was used for evaluation. The estimation accuracy of the GA-AEKF and GA-AUKF algorithms was improved by 5.1% and 6.8% respectively. This further substantiates their precision and reliability in SOC estimation. A comprehensive analysis of the aforementioned data reveals that the GA-AEKF and GA-AUKF algorithms exhibit a substantial enhancement in SOC estimation accuracy when compared to the GA-EKF algorithm. Furthermore, a comparative analysis of the robustness of GA-AEKF and GA-AUKF algorithms using MAX, MAE and RMSE indexes reveals that the GA-AUKF algorithm demonstrates superior adaptability and stability in SOC estimation of lithium-ion batteries, effectively coping with the demand for SOC estimation under complex working conditions.

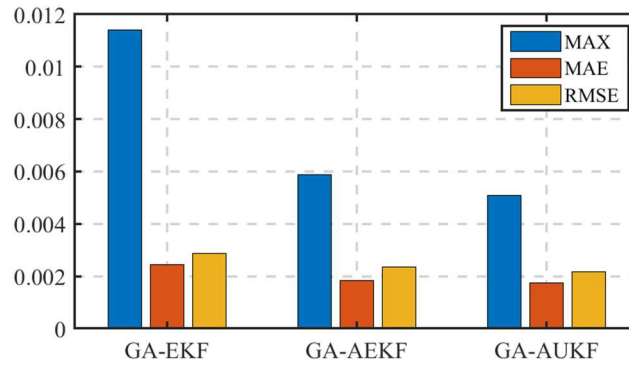


Fig. 9 Error Analysis Under EKF, AEKF and AUKF Algorithms

5. CONCLUSION

This paper takes a focus on lithium-ion batteries as the object of study, utilizing an experimental platform for conducting experiments on battery characteristics. The Thevenin model is selected as the equivalent circuit model of lithium-ion batteries. Subsequently, GA is employed for the identification of model parameters with the objective of enhancing the accuracy of the model. The identification results are effectively verified. Subsequent to the completion of parameter identification, GA-EKF, GA-AEKF and GA-AUKF were designed to achieve accurate estimation of battery SOC. The simulation and error analysis of the three algorithms were then carried out using UDDS operating

conditions data. A comparative analysis of the error results yielded by the three algorithms revealed that the GA-AUKF algorithm exhibited the optimal performance in terms of SOC estimation accuracy, with its MAX, MAE and RMSE reaching 0.51%, 0.18% and 0.22%, respectively. This outcome was found to be significantly superior to that of the GA-EKF and GA-AEKF algorithms.

ACKNOWLEDGEMENTS

This research was supported by the graduate Innovation Fund (Grant No. Y2023091) of Sichuan University of Science & Engineering. The experiments were done in the Advanced Energy Storage and Applications (AESAs) group of Beijing Institute of Technology.

REFERENCES

- [1] Lai Y W, Chi K H, Chung Y H, et al. Thermal hazard evaluation of 18650 lithium-ion batteries at various discharge rates[J]. *Journal of Loss Prevention in the Process Industries*, 2024, 89: 105323.
- [2] Wang J, Yang J, Bai W, et al. Thermal runaway and jet flame features of LIBs undergone high-rate charge/discharge: an investigation[J]. *Journal of Energy Chemistry*, 2024.
- [3] Zhang K, Zhao X, Chen Y, et al. Robust equivalent circuit model parameters identification scheme for State of Charge estimation based on maximum correntropy criterion[J]. *International Journal of Electrochemical Science*, 2024, 19(5): 100558.
- [4] Mustafa H, Bourelly C, Vitelli M, et al. SoC Estimation on Li-ion Batteries: A New EIS-based Dataset for data-driven applications[J]. *Data in Brief*, 2024, 57: 110947.
- [5] Zhou Y, Wang S, Feng R, et al. Multi-temperature capable enhanced bidirectional long short term memory-multilayer perceptron hybrid model for lithium-ion battery SOC estimation[J]. *Energy*, 2024, 312: 133596.
- [6] Kang J, Wei W, Wang Q, et al. An empirical parameter identification method considering hysteresis effects for LiFePO₄ battery's electrochemical model[J]. *Journal of Energy Storage*, 2024, 76: 109845.
- [7] Gao Ming Kun, Xu H L, Wu M B. Review of SOC estimation methods for power battery based on equivalent circuit model[J]. *Journal of Electrical Engineering*, 2021, 16(1): 90-102.
- [8] Wang Q, Gao T, Li X. SOC estimation of lithium-ion battery based on equivalent circuit model with variable parameters[J]. *Energies*, 2022, 15(16): 5829.
- [9] Xu Z, Wang J, Lund P D, et al. Co-estimating the state of charge and health of lithium batteries through combining a minimalist electrochemical model and an equivalent circuit model[J]. *Energy*, 2022, 240: 122815.
- [10] Xiao J, Xiong Y, Zhu Y, et al. Multi-innovation adaptive Kalman filter algorithm for estimating the SOC of lithium-ion batteries based on singular value decomposition and Schmidt orthogonal transformation[J]. *Energy*, 2024, 312: 133597.
- [11] Guo Y, Zhao Z, Huang L. SoC estimation of lithium battery based on AEKF algorithm[J]. *Energy Procedia*, 2017, 105: 4146-4152.
- [12] Fan X, Feng H, Yun X, et al. SOC estimation for lithium-ion battery based on AGA-optimized AUKF[J]. *Journal of Energy Storage*, 2024, 75: 109689.